Identification of small molecules that mitigate vincristine-induced neurotoxicity while sensitizing leukemia cells to vincristine

Barthelemy Diouf[1], Claudia Wing[2], John C. Panetta[1], Donnie Eddins[3], Wenwei Lin[4], Wenjian Yang[1], Yiping Fan[5], Deqing Pei[6], Cheng Cheng[6], Shannon M. Delaney[2], Wei Zhang[7], Erik J. Bonten[1], Kristine R. Crews[1], Steven W. Paugh[1], Lie Li[1], Burgess B. Freeman 3[rd8], Robert J. Autry[1], Jordan A. Beard[1], Daniel C. Ferguson[1], Laura J. Janke, DVM[9], Kirsten K. Ness[10], Taosheng Chen[4], Stanislav S. Zakharenko[3], Sima Jeha[11], Ching-Hon Pui[11], Mary V. Relling[1], M. Eileen Dolan[2], and William E. Evans[1*].

[1]Hematological Malignancies Program and Department of Pharmaceutical Sciences, St. Jude Children's Research Hospital, Memphis, Tennessee; [2] Section of Hematology/Oncology, Department of Medicine, University of Chicago, Chicago, Illinois; [3]Departmentof Developmental Neurobiology, St. Jude Children's Research Hospital, Memphis, Tennessee; [4]Department of Chemical Biology and Therapeutics, St. Jude Children's Research Hospital, Memphis, Tennessee; [5]Department of Computational Biology, St. Jude Children's Research Hospital, Memphis, Tennessee; [6] Department of Biostatistics, St. Jude Children's Research Hospital, Memphis Tennessee; [7]Department of Preventive Medicine, Northwestern University Feinberg School of Medicine, Chicago, IL; [8]Preclinical Pharmacokinetics Shared Resource, St. Jude Children's Research Hospital, Memphis, Tennessee. [9]Department of Pathology, St. Jude Children's Research Hospital, Memphis, Tennessee, [10]Department of Epidemiology and Cancer Control, St. Jude Children's Research Hospital, Memphis, Tennessee, [11]Department of Oncology, St. Jude Children's Research Hospital, Memphis, Tennessee.

[*]Correspondence: William E. Evans, St. Jude Children's Research Hospital

262 Danny Thomas Place., Memphis, TN 38105, USA, Phone: (901)595-6850,

email: william.evans@stjude.org

This article has been accepted for publication and undergone full peer review but has not been through the copyediting, typesetting, pagination and proofreading process, which may lead to differences between this version and the Version of Record. Please cite this article as doi: 10.1111/CTS.13012

Conflict of Interest statement

The authors declared no competing interests for this work.

Funding Information

This work was supported, in part, by NIH Grants R37 CA36401 (W.E.E.); U01 GM92666 (W.E.E.); R21 CA222764 (M.E.D), R01 MH097742 (S.S.Z), R01 DC012833 (S.S.Z), St. Jude Comprehensive Cancer Center Support Grant CA21765 from the National Cancer Institute; University of Chicago Comprehensive Cancer Center Women's Board (M.E.D.), University of Chicago Cancer Center Support Grant CA014599 and by ALSAC.

Disclaimer

The content is solely the responsibility of the authors and does not necessarily represent the official views of the National Institute of Health.

Keywords: vincristine neurotoxicity, leukemia cell sensitivity, translational pharmacology, drug-drug interaction, pharmacokinetics.

Abstract

Vincristine is one of the most widely prescribed medications for treating solid tumors and acute lymphoblastic leukemia (ALL) in children and adults. However, its major dose-limiting toxicity is peripheral neuropathy that can disrupt curative therapy. Peripheral neuropathy can also persist into adulthood, compromising quality of life of childhood cancer survivors. Reducing vincristine-induced neurotoxicity without compromising its anticancer effects would be ideal. Here we show that low expression of *NHP2L1*

is associated with increased sensitivity of primary leukemia cells to vincristine, and that concomitant administration of vincristine with inhibitors of NHP2L1 increases vincristine cytotoxicity in leukemia cells, prolongs survival of ALL xenograft mice, but decreases vincristine effects on human induced pluripotent stem cell (hiPSC)-derived neurons and mitigates neurotoxicity in mice. These findings offer a strategy for increasing vincristine's antileukemic effects while reducing peripheral neuropathy in patients treated with this widely prescribed medication.

Introduction

The success of drug therapy for many diseases is often compromised by adverse effects of medications used in the clinic[1,2]. This is frequently true for cancer chemotherapy, which typically have a narrow therapeutic index, damaging normal tissues at doses required for anticancer effects. Vincristine is a widely used anticancer drug that has a very narrow therapeutic index, with a dose-limiting toxicity of peripheral neuropathy, characterized by neuropathic pain and sensory and motor dysfunction[3,4], that can persist for decades after completing therapy, compromising the quality of life of cancer survivors[5]. There are currently no effective strategies for reducing vincristine-induced neurotoxicity while retaining its therapeutic efficacy. Therefore, our current work focused on elucidating strategies to improve the therapeutic index of vincristine (i.e. increase antileukemic effects relative to neurotoxicity). We found that low expression of *NHP2L1* in primary acute lymphoblastic leukemia (ALL) cells was associated with greater sensitivity to vincristine, suggesting that inhibition of NHP2L1 could increase vincristine's antileukemic effects. Because ALL cells undergo mitosis whereas neurons are post-mitotic[6,7], we hypothesized that small molecule inhibitors of NHP2L1[8], which is a component of the spliceosome complex[9-11] involved in mitosis[12], might increase the sensitivity of leukemia cells to vincristine without altering the sensitivity of neurons, thus enhancing vincristine' therapeutic index. Here we report that dipyridamole, an inhibitor of

NHP2L1, increases the sensitivity of leukemia cells to vincristine and prolongs survival of ALL xenograft mice, while protecting both human induced pluripotent stem cell (hiPSC)-derived neurons and mice from vincristine-induced neurotoxicity.

Methods

Patients.

We studied pediatric patients (age ≤21 years) with newly diagnosed ALL who were enrolled on St. Jude Total Therapy XV and XVI (Memphis, USA), and used publicly available data from the 9th ALL Dutch Childhood Oncology Group (DCOG) protocol at Erasmus Medical Center, Sophia Children's Hospital (Rotterdam, the Netherlands), or treatment protocol 92 or 97 of the German Cooperative Study Group for Childhood Acute Lymphoblastic Leukemia (COALL; Hamburg, Germany). (https://www.ncbi.nlm.nih.gov/geo/query/acc.cgi?acc=GSE649; https://www.ncbi.nlm.nih.gov/geo/query/acc.cgi?acc=GSE648), Informed consent was obtained from patients, their guardians, or both before enrollment. Leukemia cells were isolated by applying a Ficoll-Hypaque gradient to bone marrow aspirates obtained at diagnosis. Genome-wide mRNA expression in ALL cells was determined using the Affymetrix U133 microarray. Ex vivo drug sensitivity of primary ALL cells was determined using a modification of the MTT ((3-[4,5-dimethylthiazol-2-yl]-2, 5-diphenyl-tetrazoliumbromide) assay as we have described previously[13]. For the genome-wide interrogation of mitotic genes, there were 572 genes with a mitotic phenotype[12], 395 genes were represented on the Affy HGU133A expression array. The association between the expression of these genes and vincristine LC_{50} was first tested in a cohort of 92 patients in the St. Jude cohort, which led to the identification of 12 genes associated with vincristine LC_{50} with a *p-value* <0.05. Of these 12 genes, only *NHP2L1* expression was significantly associated with vincristine LC_{50} in the DCOG/COALL cohort used as validation cohort. Sensitive and resistant cells were defined the same way as previously described with sensitive cells as having a

vincristine concentration lethal to 50% of the cells (LC_{50}) of 0.391 μg /ml (0.474 μM) or less, and resistant cells as having an LC_{50} greater or equal to 1.758 μg/ml (2.131 μM)[13].

Cell culture.

The human T-lineage leukemia cell line CCRF-CEM was obtained from the American Type Culture Collection (ATCC, Manassas, VA, USA). The human pre-B leukemia cell line NALM-6 was obtained from the DSMZ-German Collection of Microorganisms and Cell Cultures GmbH (Braunschweig, Germany). The cells were authenticated using Short Tandem Repeat (STR) profiling[14]. The cells tested negative for mycoplasma (MycoAlert mycoplasma detection kit, Lonza, Alpharetta, GA USA). Cells were cultured in RPMI-1640 medium containing 2 mM glutamine and 10% (vol/vol) FBS at 37 °C with 5% CO_2.

Human iPSC-derived neurons (Peri.4U) having > 90% purity and expressing βIII-tubulin, MAP-2, peripherin and vGLUT2 were purchased from Ncardia BV (Gosselies, Belgium). All batches of iPSC-derived neurons were tested for sterility, viability, purity, and morphology by Ncardia BV. Neurons were maintained according to the manufacturers' protocol. Three independent batches of Peri.4U neurons were used including LOT#D059_PNN, LOT#424D_v1 and LOT#428D_v2M.

Animals.

All animal studies were approved by the St. Jude Animal Care and Use Committee. Male C57BL/6J mice (The Jackson Laboratory, Bar Harbor, ME USA) at 8 weeks of age were used. The mice had free access to food and water. The mice were maintained under 12h light-dark cycle.

Reagents.

Dipyridamole (Sigma-Aldrich, St. Louis, MO, USA and LKT Labs, St. Paul, MN, USA), vincristine, scopoletin, tazarotene, dihydroxyflavone (Sigma-Aldrich, St. Louis, MO, USA), quetiapine fumarate (LKT Labs, St. Paul, MN, USA and Selleck Chemicals, Houston, TX, USA), hymecromone, esculin (Selleck Chemicals, Houston, TX, USA), chir 99021 (Cayman Chemical, Ann Arbor, MI, USA), , harmaline, fisetin (Tokyo Chemical

Industry, Thermo Fisher Scientific, USA), aurintricarboxylic acid (Calbiochem, Millipore Sigma, USA), piperacillin sodium (Santa Cruz Biotechnology, Dallas, TX, USA), olmesartan medoxomil (Ark Pharm, Arlington Heights, IL, USA).

***NHP2L1* gene knockdown.**

CEM cells were infected with MISSION lentiviral transduction particles (Sigma-Aldrich, St. Louis, MO) produced from a library of sequence-verified shRNAs targeting human *NHP2L1* transcripts. The following sequence of shRNA was used to knock down the *NHP2L1* gene:

5'- CCGGCCTGAGGTTGTGTATCATATTCTCGAGAATATGATACACAACCTCAGGTTTTTG -3' (TRCN0000074798); 5'CCGGCAATCCATTCAGCAGTCCATTCTCGAGAATGGACTGCTGAATGGATTGTTTTTG-3' (TRCN0000074801). Nontarget shRNA control particles (SHC002V; Sigma-Aldrich) were also used. Individual cell clones were isolated in medium containing puromycin. Gene knocked down was assessed by western blot. Human iPSC-derived neurons, Peri.4U underwent siRNA transfection using Accell human *NHP2L1* SMARTpool siRNA and a non-targeting siRNA pool as the negative control (Dharmacon Inc., Lafayette, CO, USA). Waltham, MA, USA). Quantitative reverse transcription polymerase chain reaction (qRT-PCR) was used to measure the level of *NHP2L1* expression (SNU13, Hs03025442_s1) compared to the housekeeping control Beta-2-microglobulin (4326319E) (both from Thermo Fisher Scientific).

Western blot analysis.

Lysates from the CEM or NALM6 cell lines were separated by electrophoresis on a SDS-polyacrylamide gel. The proteins were then electroblotted onto a Hybond-P PVDF membrane. Protein expression was analyzed using the primary antibodies anti-GAPDH (Santa Cruz Biotechnology #sc-20357) and anti-NHP2L1 (Abcam #ab95958). Horseradish peroxidase–conjugated secondary antibodies were purchased

from Agilent (Santa Clara, CA, USA). Phospho-histone H3 (Ser10) clone 3H10 (Millipore #05-806); Beta tubulin (Sigma-Aldrich#C4585) Histone H3 (proteintech#17168-1-AP) were used. Sororin was provided by Dr Jan-Michael Peters from the Research Institute of Molecular Pathology, Vienna.

High content imaging of neuronal morphological characteristics.

After drug treatment, neurons were stained with 5μg/mL Hoechsts 33342 (Sigma Aldrich) and 10μg/mL Calcein AM (Molecular Probes, ThermoFisher Scientific, Waltham, MA, USA) for 10 minutes at room temperature. Imaging was performed at 10x magnification using an ImageXpress Micro imaging device (Molecular Devices, LLC, Sunnyvale, CA, USA) at the University of Chicago Cellular Screening Center. The MetaXpress software Neurite Outgrowth Application Module was utilized to collect individual cell measurements of mean/median/maximum process length, total neurite outgrowth (the sum of the length of all processes), number of processes, number of branches, cell body area, mean outgrowth intensity, straightness and cell number. A minimum of 1000 cells per condition were imaged in each of the five independent experiments.

Gene expression in the iPSC-derived neurons Peri.4U.

Total RNA from iPSC-derived neurons Peri. 4U was extracted and prepared as previously described[15]. Samples were evaluated on the Affymetrix GeneChip Human Transcriptome (HTA) 2.0 Array (Affymetrix, Santa Clara, CA) and data generated at the University of Chicago Genomics Core. The raw data were processed using the Affymetrix Power Tools (APT) (v1.16) and the HTA 2.0 array annotation library (release 1.0). Background subtraction, normalization, and probe-set summarization were performed using the APT software. Briefly, gene-level data were background corrected and normalized using the Robust Multi-array Average method on perfectly matched probes through median polish[16]. The summarized gene-level data were $\log_2$ transformed for downstream analysis.

Cell viability assay.

HiPSC-derived neurons cell viability was assessed at 72 hours post drug treatment by the Cell Titer-Glo 2.0 assay (Promega, Madison, WI, USA) which measures ATP.

***Ex vivo* drug sensitivity (MTT) assay.**

Ex vivo drug sensitivity of CEM and NALM6 cell lines was determined using a modification of the MTT ((3-[4,5-dimethylthiazol-2-yl]-2, 5-diphenyl-tetrazoliumbromide) assay as described previously[13]. Briefly, cells in mid-log phase were exposed to serial dilutions of the different drugs and analyzed after three days of incubation. The concentration of drug required for 50% cell kill (LC_{50}) was used as the measure of relative sensitivity to each compound.

Synergy studies: Response Surface Modeling.

A modification of the response surface modeling approach[17-19] implemented in Matlab (version R2019a, Mathworks, Natick, MA) was used to determine changes in the response of two drugs given in combination from an additive response. A drug combination was considered either synergistic or antagonistic if α, the interaction term describing the change in response relative to the additive model, was either positive or negative, respectively. We quantified the effects of vincristine in the presences of a fixed concentration of the second drug as the ratio of the estimated additive EC_{50} to estimated actual EC_{50} of vincristine and the fixed concentration of the second drug.

Intracellular concentration of vincristine and dipyridamole in leukemia cell lines and in hiPSC-derived neurons.

After treatment with vincristine and dipyridamole, the cells were harvested, washed twice with Hank's Balanced Salt Solution (HBSS, Sigma Aldrich), pelleted and stored at -80^{o}C. The cells were later resuspended in HBSS, sonicated to fully lyse the cells, and after centrifugation the supernatant was

collected. Quantitation of analytes was carried out with a Waters ACQUITY separation system (Waters Corp, Milford, MA, USA) and Xevo TQ triple-quadrupole system (Beverly, MA, USA). Separation was achieved on a Waters ACQUITY $BEHC_{18}$ column (1.7 μm, 50x2.1mm) using a column heater operating at 40°C with Waters ACQUITY in-line filter. Autosampler temperature was maintained at 15 °± 5 °C. The gradient mobile phase was composed of acetonitrile (B) and 15mM ammonium acetate in 0.02% formic acid wáter (A). The flow rate was 0.6 ml/min and the separation was completed within 6 minutes. The instrument was equipped with an electrospray interface, and was controlled by Masslynx 4.1 software (Waters). The analysis was performed in MRM mode: *m/z* 505.46>429.27 for dipyridamole, *m/z* 525.6>449.3 for dipyridamole_d3; *m/z* 825.36>807.39 for vincristine, and *m/z* 828.56>810.57 for vincristine_d3. The MS/MS conditions were as follows: capillary voltage: 0.5kV; source temperature: 150°C; desolvation temperature: 600°C; cone gas flow:0 l/h; desolvation gas flow: 1000 l/h.

Vincristine (VCR) Intracellular Concentration Modeling.

Vincristine intracellular ($VCR_{intracellular}$) concentrations with respect to vincristine and dipyridamole (DIP) extracellular concentration and incubation time were modeled with the following multivariate Hill function:

$$VCR_{intracellular} = \frac{[V_{max} + DIP \cdot \Delta V_{max}]t^n}{[K_M + DIP \cdot \Delta K_M]^n + t^n}$$

For each of the two extracellular concentrations of vincristine [2 nM (1.65 μg/L) and 40 nM (33 μg/L)] the dependent variables V_{max}, K_M, n, ΔV_{max}, and ΔK_M were estimated relative to the two independent variables dipyridamole: extracellular concentration of dipyridamole [0 μM, 2.5 μM (1.265 mg/L), 5 μM (2.525 mg/L), 10 μM (5.05 mg/L] and the incubation time t (1, 6, 12, and 24 hours). If the parameters ΔV_{max} or ΔK_M were significantly different from zero then the effect of dipyridamole concentration significantly altered the steady-state intracellular concentration of VCR.

Dipyridamole (DIP) Intracellular Concentration Modeling.

Dipyridamole intracellular ($DIP_{intracellular}$) concentration with respect to vincristine (VCR) and dipyridamole extracellular concentration and incubation time were modeled with the following multivariate linear function.

$$DIP_{intracellular} = [b + \Delta b \cdot VCR] + [m + \Delta m \cdot VCR] \cdot t$$

For each of the three extracellular concentrations of dipyridamole [0 μM, 2.5 μM (1.265 mg/L), 5 μM (2.525 mg/L), 10 μM (5.05 mg/L)] the dependent variables *b, m, ⊿b,* and *⊿m* were estimated relative to the two independent variables vincristine: extracellular concentration of vincristine [0, 2 nM (1.65 μg/L), and 40 nM (33 μg/L)] and the incubation time t (1, 6, 12, and 24 hrs). If the parameters *⊿b* or *⊿m* were significantly different from zero then the effect of vincristine concentration significantly altered the steady-state intracellular concentration of dipyridamole

***In vivo* pharmacokinetic studies.**

Methods for the in vivo pharmacokinetics studies performed in mice are provided in the Supplementary methods.

Mouse neurotoxicity assessment: Mechanical allodynia. Mice were acclimated before testing. The mice were treated, from day 1 to day 10, intraperitoneally with vincristine or saline and by oral gavage with dipyridamole or the vehicle of dipyridamole (1% methylcellulose and 1% Tween 80, pH adjusted to 2.0 with HCl). Mechanical allodynia was evaluated in mice using von Frey filaments (0.16 g, 0.4 g, 0.6 g, 1 g

and 2 g) prior to drug treatment, at days 7 and 10 of drug administration, and at day 14 (4 days after discontinuation of treatment). Each mouse was tested ten times in increasing order of filament force. The data obtained from three different replicate experiments comprise both cross-sectional and time-series measurements of responses to stimulus under multiple conditions. The withdraw threshold (g) was determined as the minimal force filament for which a response was obtained at least five times out of the ten stimulations.

Statistical analyses

Student's t-test was used to compare the means between two different experimental conditions.

Analyses were done using SAS, version 9.4 (Cary, NC), R (The R Project http://www.r-project.org/) and SigmaPlot 11.0 (Systat Software. Inc, San Jose, CA).

Statistical analyses of longitudinal *in vivo* data in mice accounted for possible between-subject heterogeneity and within-subject correlation. The longitudinal mean response was modeled by a mixed effect linear model, with treatment group, filament level, baseline response and batch as fixed effects and a random effect to account for intra-animal longitudinal correlation with compound symmetry working covariance structure. The primary effect of interest was a comparison of neuropathy events among the treatment groups. To visually depict the cross-sectional and cumulative proportion (CPN) of mice positive for neuropathy (NP+) in each treatment group, we dichotomized the response [NP+ vs negative for neuropathy (NP-)] using a threshold of the 95^{th} percentile of the percentage of response of the von Frey measurement at the baseline in all treatments and filament levels pooled. Any measurement above or equal to this threshold was defined as NP+. The 95^{th} percentile of the von Frey measurements in all treatments pooled together was 90, thus any von Frey measurement exceeding 90 defined a positive finding for neuropathy (NP+). Neuropathy was assessed at Days 7, 10 and 14, with the day of the first measurement ≥90 defining the time to the first NP+ event in the cumulative proportion analysis and

figure. In the mouse ALL xenograft survival study, all mice reached the study endpoint by the time of data freeze, therefore no observed survival time was censored. Survival time distributions were compared using exact Wilcoxon rank sum test between the different treatment groups.

Results

NHP2L1 expression and vincristine LC_{50} in primary leukemia cells.

In a genome-wide interrogation of genes whose mRNA expression was significantly related to the sensitivity of primary ALL cells to vincristine (LC_{50}), we identified *NHP2L1* expression as the top mitosis-related [12] gene significantly associated with vincristine LC_{50} in two different patient cohorts (Table S1). Specifically, lower *NHP2L1* mRNA expression in leukemia cells isolated from diagnostic bone marrow aspirates of children with newly diagnosed ALL was significantly associated with increased sensitivity to vincristine in B cell and T cell leukemia in two patient cohorts (Figures 1a-b).

NHP2L1 knockdown and vincristine LC_{50} in leukemia cells.

To determine whether a low level of *NHP2L1* expression increased leukemia cell sensitivity to vincristine, we reduced the expression of NHP2L1 by infecting two human leukemia cells (the T-lineage cell line CCRF-CEM and the B-lineage NALM6 cell lines) with shRNA against *NHP2L1*. As shown in Figures 2a-c, the knockdown of *NHP2L1* using two different shRNA clones resulted in a significant reduction in NHP2L1 protein and significantly increased sensitivity of human CCRF-CEM and NALM6 ALL cells to vincristine (Figures 2b-d), consistent with the association of lower NHP2L1 expression with greater vincristine sensitivity (low LC_{50}) in primary leukemia cells isolated from patients with newly diagnoses ALL (Figure 1).

***NHP2L1* knockdown and vincristine-induced accumulation of mitotic cells.**

To assess the mechanisms by which NHP2L1 influences vincristine-induced cell death through mitotic arrest, we assessed the effects of vincristine on HISTONE H3 phosphorylation at serine 10 [Phospho-HISTONE H3 (Ser10)], a mitosis marker[20], in CEM and in NALM6 cells. We documented increased vincristine-induced HISTONE H3 phosphorylation (Ser10) after *NHP2L1* knockdown (Figures 2e-h), indicating that knockdown of *NHP2L1* sensitizes cells to the microtubule inhibitor vincristine in part by inducing mitotic arrest.

Small molecule inhibitors of NHP2L1-U4 interaction synergize with vincristine in leukemic cells.

NHP2L1's known function is via interaction with the spliceosome component U4 RNA. We developed an assay based on time-resolved FRET (TR-FRET) to detect the interaction between NHP2L1 and U4 5'-stem loop (5'-SL) and used this to conduct a high-throughput screen (HTS) for small molecules inhibiting this interaction[8]. Given the greater vincristine sensitivity of primary ALL cells with lower NHP2L1 expression, we hypothesized that inhibitors of the NHP2L1-U4 interaction would potentiate the effects of vincristine in ALL cells. We further assessed the effects of several small molecule hits in this analysis (scopoletin, quetiapine fumarate, hymecromone, harmaline, fisetin, esculin, dihydroxyflavone, chir 99021, aurintricarboxylic acid, tazarotene, dipyridamole, piperacillin sodium, olmesartan medoxomil) on vincristine sensitivity in human leukemic cells. Synergistic effects between these small molecules and vincristine were assessed by the response surface modeling method[17-19] (based on α). This revealed that dipyridamole, tazarotene, and quetiapine fumarate synergize with vincristine cytotoxicity in human leukemia CEM cells (Figures S1a-m). We also validated these results in a second human leukemia cell line, NALM6, with dipyridamole providing the highest level of synergy (Figures S1n-r) (Table 1).

Effects of these small molecules on vincristine-induced neurotoxicity in human iPSC-derived neurons.

To assess the effects of these small molecules on vincristine-induced neurotoxicity, we used neurons derived from human iPSCs. These hiPSC-derived neurons were previously validated as a model to evaluate chemotherapy-induced neurotoxicity[21,22] including vincristine-induced neurotoxicity[23]. In contrast to ALL cells, we documented significantly greater resistance of hiPSC-derived neurons to vincristine in the presence of these small molecules (Table 2). This protection against vincristine-induced toxicity in neurons was evidenced by the antagonistic effects of these small molecules as measured by neurite outgrowth, branches, processes and cytotoxicity compared to vincristine alone (Table 2), whereas knockdown of *NHP2L1* in hiPSC-derived neurons did not have any effect on these morphologic phenotypes (Figure S2). Overall, our results show that dipyridamole, quetiapine fumarate and tazarotene synergized with vincristine in leukemia cells but mitigated vincristine effects on neurons (Figure S3). Because dipyridamole showed the strongest degree of synergy with vincristine in leukemia cells and protection against vincristine toxicity in iPSC-derived neurons, as documented for hiPSC-derived neurons outgrowth and ability to expand in branches and processes (Figures 3a, 3b; Figure S4), dipyridamole was chosen for further experiments.

Mechanisms by which dipyridamole alters vincristine effects in ALL cells and in neurons.

To understand the mechanisms by which dipyridamole influences vincristine-induced cell death, we assessed the effect of vincristine on Histone H3 phosphorylation in the presence of increasing concentration of dipyridamole in CEM and in NALM6 leukemia cells. Dipyridamole induced a dose-dependent increase in phospho-histone H3 (Ser10) levels in CEM (Figures 4a and 4b) and in NALM6 cells (Figures 4c and 4d), consistent with the increased accumulation of mitotic cells prior to vincristine-induced cell death. The primary function of NHP2L1 through its interaction with U4 involves the splicing of SORORIN pre-mRNA. Disruption of this interaction compromises SORORIN splicing and decreases the abundance of mature SORORIN protein[24]. We documented a dose dependent effect of dipyridamole on

SORORIN protein levels, with the highest concentration of dipyridamole [10μM(5.05mg/L)] producing the lowest level of SORORIN protein in CEM (Figures 4e and 4f) and in NALM6 cells (Figures 4g and 4h), consistent with dipyridamole exerting its effects via interference with NHP2L1/U4 interaction.

Because dipyridamole is a known inhibitor of the ABCB1 efflux transporter, we assessed the effects of dipyridamole on the intracellular concentration of vincristine and vice versa. There was a significant increase in the intracellular concentration of vincristine with increasing concentrations of dipyridamole in CEM (Figure 5a) and in NALM6 leukemia cells (Figure S5a), indicating that dipyridamole can also affect sensitivity of leukemia cells by increasing the intracellular concentration of vincristine. In contrast, increasing concentrations of vincristine did not significantly increase the intracellular concentration of dipyridamole in CEM (Figure 5b) or in NALM6 cells (Figure S5b). We also assessed the intracellular concentrations of dipyridamole and vincristine in hiPSC-derived neurons, documenting that dipyridamole did not increase vincristine intracellular concentrations (Figures 5c and 5d), but instead trended toward lower vincristine intracellular concentrations in the presence of dipyridamole in hiPSC-derived neurons. Gene expression analyses indicated low expression of *ABCB1* (relative to other transporters), the main efflux transporter of vincristine, in hiPSC-derived neurons but not in the leukemia cells (Tables S2-3).

***In vivo* pharmacokinetic (PK) studies.**

Pharmacokinetic studies verified that mice had clinically relevant plasma drug concentrations with doses of vincristine 0.1 mg/kg intraperitoneal and dipyridamole 200 mg/kg PO. These studies documented total plasma concentrations of vincristine and dipyridamole of up to 10 ng/ml (12.1 nM) and 5000 ng/mL (9.9 μM), respectively. Clinically studies have reported plasma concentrations up to 31.2 ng/mL (37.8 nM) for vincristine[25] and 6000 ng/mL (11.9 μM) for dipyridamole[26]. There was no significant difference in vincristine systemic clearance in mice treated with vincristine and dipyridamole versus vincristine alone (4.88 L/hr/kg versus 5.96 L/hr/kg respectively (p=0.153) (Figure S6a). Likewise, concomitant vincristine

administration did not significantly affect the apparent oral clearance or plasma exposure of oral dipyridamole in mice *(p*=0.950) (Figure S6b). Overall, these data indicate that concomitant dipyridamole 200mg/kg PO daily does not affect vincristine clearance or plasma exposure in mice.

***In vivo* effects of dipyridamole on vincristine-induced peripheral neuropathy and on vincristine's antileukemic effects in a mouse xenograft model.**

To determine whether dipyridamole alters vincristine-induced peripheral neuropathy in mice, we used von Frey filaments[27]. We compared the percentage paw withdrawal response as a measure of neurotoxicity in mice among four different treatment groups of mice, using a mixed effect model with baseline response, filament strength, and measurement time point as covariates in the analysis. We observed a significant increase in paw withdrawal responses of mice receiving vincristine alone. Importantly, the administration of dipyridamole with vincristine significantly lowered this response (Figure 5e, Figures S6c-f, and Table S4), indicating *in vivo* mitigation of the neurotoxic effects of vincristine. These results were confirmed by a significantly higher cumulative incidence of cutaneous pain sensitivity (Figure 5f) and a significant decrease in mechanical sensitivity threshold in mice receiving vincristine alone compared to mice treated with vincristine and dipyridamole (Figure S6g), consistent with neuroprotective effects of dipyridamole observed in the human iPSC-derived neurons. Using NSG mice inoculated with human CEM leukemia cells we documented that dipyridamole significantly prolonged the survival of mice treated with vincristine (Figure 5g) consistent with the synergistic effects of dipyridamole and vincristine seen in leukemia cells *ex vivo*.

Discussion

The sensitivity of primary leukemia cells to antileukemic agents, measured in *ex vivo* assays as LC_{50}, is a good predictor of *in vivo* drug response in patients with ALL[13,28,29]. In a genome-wide interrogation study based on the sensitivity of primary ALL cells to vincristine, we discovered that low expression of *NHP2L1* is associated with increased sensitivity to vincristine and this was validated by manipulating *NHP2L1* in human ALL cell lines. Vincristine exerts its antileukemic effects by interfering with microtubule formation and mitotic spindle dynamics[30-32], thereby inducing mitotic arrest and apoptosis[33]. Low NHP2L1 is also associated with mitotic arrest[24], consistent with low expression of NHP2L1 sensitizing ALL cells to vincristine, as both increase accumulation of mitotic cells. Previous studies have shown synergistic effects between antimitotic drugs such as vincristine and proteins involved in mitosis[34-36]. We previously identified FDA-approved small molecule that are inhibitors of NHP2L1 function, and here we documented synergy between vincristine and several of these NHP2L1 inhibitors, including tazarotene, quetiapine fumarate and dipyridamole. Tazarotene is an acetylenic retinoid used for the topical treatment of acne and psoriasis[37]. Quetiapine fumarate is an antipsychotic used in the treatment of depression, schizophrenia and bipolar disorder[38]. Dipyridamole inhibits platelet aggregation and thrombus formation and is widely used clinically as an antiplatelet drug with no major side-effects [39].

We further documented that dipyridamole decreases the cellular level of SORORIN, a protein that requires normal spliceosome (NHP2L1) function to maintain adequate cellular levels to regulate sister chromatid cohesion during mitosis[40]. Mitotic arrest could be caused by either defects in mitotic spindle dynamics caused by vincristine and (or) defects in sister chromatid cohesion following reduction of SORORIN protein level[24,41,42]. We also observed increased intracellular concentrations of vincristine in leukemia cells when ALL cells were treated concomitantly with dipyridamole. Vincristine is transported out of leukemia cells mainly by the multidrug efflux pump P-glycoprotein (Pgp, encoded by *ABCB1*)[43,44]. Dipyridamole is a well-known inhibitor of P-glycoprotein[45] and dipyridamole has been shown to increase the intracellular concentration of Pgp substrates[45-47] consistent with the increased level of vincristine in

leukemia cells treated with dipyridamole. Dipyridamole did not increase the intracellular concentration of vincristine in hiPSC neurons, perhaps due to the low constitutive expression of ABCB1 in hiPSC-derived neurons. We have not assessed the impact of differences in plasma proteins, which is unlikely to be substantial given the modest (around 75%) plasma protein binding of vincristine[48].

Low expression or knockdown of *NHP2L1* increased sensitivity of leukemic cells to vincristine, whereas, knockdown of *NHP2L1* did not have any effect on vincristine mediated toxicity in iPSC-derived neurons. The differing effect of NHP2L1 on ALL cells versus hiPSC-derived neurons is likely also because neurons are post-mitotic cells and NHP2L1 acts primarily on mitotic cells. Thus, there are at least two potential reasons why dipyridamole has different effects on vincristine in leukemia cells versus hiPSC-derived neurons: (1) dipyridamole increases intracellular vincristine by inhibiting the efflux transporter (ABCB1) in ALL cells but not in iPSC-derived neurons, and (2) the inhibition of NHP2L1 has different consequences in cells undergoing mitosis (ALL) versus post-mitotic cells such as neurons. We cannot exclude the possibility of other mechanisms by which dipyridamole differentially alters vincristine sensitivity in leukemia cells and hiPSC-derived neurons, as it is known to have several additional properties (anti-oxidant and anti-inflammatory)[49,50].

We have previously identified an inherited variant in *CEP72*, which encodes a protein essential for microtubule formation that increases the risk and severity of vincristine-induced acute neuropathy[23], providing a strategy for identifying patients at highest risk of this common toxicity. Our present discovery of small molecules capable of increasing the sensitivity of ALL cells to vincristine and prolonging survival of mice bearing human leukemia cells while simultaneously protecting neurons from vincristine-induced neurotoxicity constitutes another step toward improving the efficacy while mitigating the neurotoxicity of vincristine.

In conclusion, we have shown that dipyridamole, a small molecule inhibitor of NHP2L1, synergizes with vincristine in leukemic cells while mitigating vincristine-induced neurotoxicity, opening the possibility of improving the therapeutic index of this widely prescribed anticancer agent, which will require a prospective clinical trial to validate in patients.

Study Highlights

What is the current knowledge on the topic?

Vincristine is a widely prescribed drug, but its use is limited by its main side effect, neurotoxicity. There are currently no strategies to increase vincristine efficacy while mitigating its neurotoxic effects.

What question did this study address?

How to improve vincristine efficacy while reducing its main side effect, neurotoxicity?

What this study adds to our knowledge?

The present study shows for the first time the possibility of reduced vincristine-induced neurotoxicity while improving vincristine anti-leukemia effect by using small molecules.

How this might change clinical pharmacology or translational science?

The current translational study will permit a safer and more efficient use of vincristine.

Acknowledgements

We thank Dr Jan-Michael Peters (Research Institute of Molecular Pathology, Vienna) for providing SORORIN antibody. We thank Siamac Sahely, John Stukenborg, Hannah Williams, Sean Savage, Michael Anderson, Chandra Savage, Kerry Heath, Jack Carpenter, Cara Goodrum, Madoka Inoue, Yingzhe Wang, for their technical assistance with experiments. We thank Jerry Harris, Elizabeth Stevens and Joshua

Stokes for preparation of the figures. We thank the Shared Research Resources of the St. Jude Comprehensive Cancer Center for imaging and gene-expression profiling and the St. Jude Children's Research Hospital Animal Resource Center for husbandry and the Cellular Screening Center and the Genomics Cores at the University of Chicago for use of the ImageXpress and gene array processing, respectively.

Authors Contributions

B.D., and W.E.E. designed the research. B.D., C.W., D.E., W.L., S.M.D., and I.I., performed the research. B.D., C.W., J.C.P., D.E., W.Y., Y.F., D.P., C.C., B.B.F., and L.J.J., analyzed the data. B.D., W.E.E., M.E.D., M.V.R., C.H.P., S.J., R.P., M.L.D.B., S.S.Z., and T.C., supervised the research. B.D., and W.E.E., wrote the manuscript with the help from the other authors. B.D., C.W., J.C.P., D.E., W.L., W.Y., Y.F., D.P., C.C., S.M.D., W.Z., E.J.B., K.R.C., S.W.P., L.L., B.B.R., R.J.A., J.A.B., D.C.F., L.J.J., K.K.N., T.C., S.S.Z., S.J., C.H.P., M.V.R., M.E.D., and W.E.E., reviewed the manuscript.

References

1 Calcabrini, C., Maffei, F., Turrini, E. & Fimognari, C. Sulforaphane Potentiates Anticancer Effects of Doxorubicin and Cisplatin and Mitigates Their Toxic Effects. *Frontiers in pharmacology* **11**, 567, doi:10.3389/fphar.2020.00567 (2020).

2 Alam, M., Yadav, R. K., Minj, E., Tiwari, A. & Mehan, S. Exploring molecular approaches in Amyotrophic lateral sclerosis: Drug targets from clinical and pre-clinical findings. *Current molecular pharmacology*, doi:10.2174/1566524020666200427214356 (2020).

3 Bradley, W. G., Lassman, L. P., Pearce, G. W. & Walton, J. N. The neuromyopathy of vincristine in man. Clinical, electrophysiological and pathological studies. *Journal of the neurological sciences* **10**, 107-131, doi:10.1016/0022-510x(70)90013-4 (1970).

4 Gidding, C. E. *et al.* Vincristine pharmacokinetics after repetitive dosing in children. *Cancer chemotherapy and pharmacology* **44**, 203-209, doi:10.1007/s002800050968 (1999).

5 Bjornard, K. L. *et al.* Peripheral neuropathy in children and adolescents treated for cancer. *The Lancet. Child & adolescent health* **2**, 744-754, doi:10.1016/s2352-4642(18)30236-0 (2018).

6 Ghelli Luserna di Rorà, A., Martinelli, G. & Simonetti, G. The balance between mitotic death and mitotic slippage in acute leukemia: a new therapeutic window? *Journal of hematology & oncology* **12**, 123, doi:10.1186/s13045-019-0808-4 (2019).

7 Iwata, R., Casimir, P. & Vanderhaeghen, P. Mitochondrial dynamics in postmitotic cells regulate neurogenesis. *Science (New York, N.Y.)* **369**, 858-862 (2020).

8 Diouf, B. *et al.* Alteration of RNA Splicing by Small-Molecule Inhibitors of the Interaction between NHP2L1 and U4. *SLAS discovery : advancing life sciences R & D* **23**, 164-173, doi:10.1177/2472555217735035 (2018).
9 Liu, S. *et al.* Binding of the human Prp31 Nop domain to a composite RNA-protein platform in U4 snRNP. *Science (New York, N.Y.)* **316**, 115-120, doi:10.1126/science.1137924 (2007).
10 Falb, M., Amata, I., Gabel, F., Simon, B. & Carlomagno, T. Structure of the K-turn U4 RNA: a combined NMR and SANS study. *Nucleic acids research* **38**, 6274-6285, doi:10.1093/nar/gkq380 (2010).
11 Vidovic, I., Nottrott, S., Hartmuth, K., Lührmann, R. & Ficner, R. Crystal structure of the spliceosomal 15.5kD protein bound to a U4 snRNA fragment. *Molecular cell* **6**, 1331-1342, doi:10.1016/s1097-2765(00)00131-3 (2000).
12 Neumann, B. *et al.* Phenotypic profiling of the human genome by time-lapse microscopy reveals cell division genes. *Nature* **464**, 721-727, doi:10.1038/nature08869 (2010).
13 Holleman, A. *et al.* Gene-expression patterns in drug-resistant acute lymphoblastic leukemia cells and response to treatment. *The New England journal of medicine* **351**, 533-542, doi:10.1056/NEJMoa033513 (2004).
14 Stabley, D. L. *et al.* Establishing a reference dataset for the authentication of spinal muscular atrophy cell lines using STR profiling and digital PCR. *Neuromuscular disorders : NMD* **27**, 439-446, doi:10.1016/j.nmd.2017.02.002 (2017).
15 Morrison, G. *et al.* Evaluation of inter-batch differences in stem-cell derived neurons. *Stem cell research* **16**, 140-148, doi:10.1016/j.scr.2015.12.025 (2016).
16 Irizarry, R. A. *et al.* Exploration, normalization, and summaries of high density oligonucleotide array probe level data. *Biostatistics (Oxford, England)* **4**, 249-264, doi:10.1093/biostatistics/4.2.249 (2003).
17 Greco, W. R., Bravo, G. & Parsons, J. C. The search for synergy: a critical review from a response surface perspective. *Pharmacological reviews* **47**, 331-385 (1995).
18 Minto, C. F. *et al.* Response surface model for anesthetic drug interactions. *Anesthesiology* **92**, 1603-1616, doi:10.1097/00000542-200006000-00017 (2000).
19 Jonker, D. M., Visser, S. A., van der Graaf, P. H., Voskuyl, R. A. & Danhof, M. Towards a mechanism-based analysis of pharmacodynamic drug-drug interactions in vivo. *Pharmacology & therapeutics* **106**, 1-18, doi:10.1016/j.pharmthera.2004.10.014 (2005).
20 Abdelfattah, N. *et al.* MiR-584-5p potentiates vincristine and radiation response by inducing spindle defects and DNA damage in medulloblastoma. *Nature communications* **9**, 4541, doi:10.1038/s41467-018-06808-8 (2018).
21 Wheeler, H. E., Wing, C., Delaney, S. M., Komatsu, M. & Dolan, M. E. Modeling chemotherapeutic neurotoxicity with human induced pluripotent stem cell-derived neuronal cells. *PloS one* **10**, e0118020, doi:10.1371/journal.pone.0118020 (2015).
22 Wing, C. *et al.* Application of stem cell derived neuronal cells to evaluate neurotoxic chemotherapy. *Stem cell research* **22**, 79-88, doi:10.1016/j.scr.2017.06.006 (2017).
23 Diouf, B. *et al.* Association of an inherited genetic variant with vincristine-related peripheral neuropathy in children with acute lymphoblastic leukemia. *Jama* **313**, 815-823, doi:10.1001/jama.2015.0894 (2015).
24 Sundaramoorthy, S., Vázquez-Novelle, M. D., Lekomtsev, S., Howell, M. & Petronczki, M. Functional genomics identifies a requirement of pre-mRNA splicing factors for sister chromatid cohesion. *The EMBO journal* **33**, 2623-2642, doi:10.15252/embj.201488244 (2014).
25 Moore, A. S. *et al.* Vincristine pharmacodynamics and pharmacogenetics in children with cancer: a limited-sampling, population modelling approach. *Journal of paediatrics and child health* **47**, 875-882, doi:10.1111/j.1440-1754.2011.02103.x (2011).

26 Willson, J. K. *et al.* Phase I clinical trial of a combination of dipyridamole and acivicin based upon inhibition of nucleoside salvage. *Cancer research* **48**, 5585-5590 (1988).

27 Chaplan, S. R., Bach, F. W., Pogrel, J. W., Chung, J. M. & Yaksh, T. L. Quantitative assessment of tactile allodynia in the rat paw. *Journal of neuroscience methods* **53**, 55-63, doi:10.1016/0165-0270(94)90144-9 (1994).

28 Hongo, T., Yajima, S., Sakurai, M., Horikoshi, Y. & Hanada, R. In vitro drug sensitivity testing can predict induction failure and early relapse of childhood acute lymphoblastic leukemia. *Blood* **89**, 2959-2965 (1997).

29 Kaspers, G. J. *et al.* In vitro cellular drug resistance and prognosis in newly diagnosed childhood acute lymphoblastic leukemia. *Blood* **90**, 2723-2729 (1997).

30 Jordan, M. A. & Wilson, L. Microtubules as a target for anticancer drugs. *Nature reviews. Cancer* **4**, 253-265, doi:10.1038/nrc1317 (2004).

31 Jordan, M. A., Toso, R. J., Thrower, D. & Wilson, L. Mechanism of mitotic block and inhibition of cell proliferation by taxol at low concentrations. *Proceedings of the National Academy of Sciences of the United States of America* **90**, 9552-9556, doi:10.1073/pnas.90.20.9552 (1993).

32 Toh, H. C., Sun, L., Koh, C. H. & Aw, S. E. Vinorelbine induces apoptosis and caspase-3 (CPP32) expression in leukemia and lymphoma cells: a comparison with vincristine. *Leukemia & lymphoma* **31**, 195-208, doi:10.3109/10428199809057599 (1998).

33 Blajeski, A. L., Phan, V. A., Kottke, T. J. & Kaufmann, S. H. G(1) and G(2) cell-cycle arrest following microtubule depolymerization in human breast cancer cells. *The Journal of clinical investigation* **110**, 91-99, doi:10.1172/jci13275 (2002).

34 Hugle, M., Belz, K. & Fulda, S. Identification of synthetic lethality of PLK1 inhibition and microtubule-destabilizing drugs. *Cell death and differentiation* **22**, 1946-1956, doi:10.1038/cdd.2015.59 (2015).

35 Ikezoe, T. *et al.* A novel treatment strategy targeting polo-like kinase 1 in hematological malignancies. *Leukemia* **23**, 1564-1576, doi:10.1038/leu.2009.94 (2009).

36 Tannous, B. A. *et al.* Effects of the selective MPS1 inhibitor MPS1-IN-3 on glioblastoma sensitivity to antimitotic drugs. *Journal of the National Cancer Institute* **105**, 1322-1331, doi:10.1093/jnci/djt168 (2013).

37 Tang-Liu, D. D., Matsumoto, R. M. & Usansky, J. I. Clinical pharmacokinetics and drug metabolism of tazarotene: a novel topical treatment for acne and psoriasis. *Clinical pharmacokinetics* **37**, 273-287, doi:10.2165/00003088-199937040-00001 (1999).

38 Chang, K. *et al.* Neurofunctional Correlates of Response to Quetiapine in Adolescents with Bipolar Depression. *Journal of child and adolescent psychopharmacology* **28**, 379-386, doi:10.1089/cap.2017.0030 (2018).

39 Gresele, P., Momi, S. & Falcinelli, E. Anti-platelet therapy: phosphodiesterase inhibitors. *British journal of clinical pharmacology* **72**, 634-646, doi:10.1111/j.1365-2125.2011.04034.x (2011).

40 Valcárcel, J. & Malumbres, M. Splicing together sister chromatids. *The EMBO journal* **33**, 2601-2603, doi:10.15252/embj.201489988 (2014).

41 Oka, Y. *et al.* UBL5 is essential for pre-mRNA splicing and sister chromatid cohesion in human cells. *EMBO reports* **15**, 956-964, doi:10.15252/embr.201438679 (2014).

42 Watrin, E., Demidova, M., Watrin, T., Hu, Z. & Prigent, C. Sororin pre-mRNA splicing is required for proper sister chromatid cohesion in human cells. *EMBO reports* **15**, 948-955, doi:10.15252/embr.201438640 (2014).

43 Safa, A. R., Glover, C. J., Meyers, M. B., Biedler, J. L. & Felsted, R. L. Vinblastine photoaffinity labeling of a high molecular weight surface membrane glycoprotein specific for multidrug-resistant cells. *The Journal of biological chemistry* **261**, 6137-6140 (1986).

44 Cornwell, M. M., Safa, A. R., Felsted, R. L., Gottesman, M. M. & Pastan, I. Membrane vesicles from multidrug-resistant human cancer cells contain a specific 150- to 170-kDa protein detected by photoaffinity labeling. *Proceedings of the National Academy of Sciences of the United States of America* **83**, 3847-3850, doi:10.1073/pnas.83.11.3847 (1986).
45 Verstuyft, C. *et al.* Dipyridamole enhances digoxin bioavailability via P-glycoprotein inhibition. *Clinical pharmacology and therapeutics* **73**, 51-60, doi:10.1067/mcp.2003.8 (2003).
46 Hirose, M., Takeda, E., Ninomiya, T., Kuroda, Y. & Miyao, M. Synergistic inhibitory effects of dipyridamole and vincristine on the growth of human leukaemia and lymphoma cell lines. *British journal of cancer* **56**, 413-417, doi:10.1038/bjc.1987.216 (1987).
47 Shalinsky, D. R., Slovak, M. L. & Howell, S. B. Modulation of vinblastine sensitivity by dipyridamole in multidrug resistant fibrosarcoma cells lacking mdr1 expression. *British journal of cancer* **64**, 705-709, doi:10.1038/bjc.1991.385 (1991).
48 Donigian, D. W. & Owellen, R. J. Interaction of vinblastine, vincristine and colchicine with serum proteins. *Biochemical pharmacology* **22**, 2113-2119, doi:10.1016/0006-2952(73)90110-x (1973).
49 Ciacciarelli, M., Zerbinati, C., Violi, F. & Iuliano, L. Dipyridamole: a drug with unrecognized antioxidant activity. *Current topics in medicinal chemistry* **15**, 822-829, doi:10.2174/1568026615666150220111942 (2015).
50 Balakumar, P. *et al.* Classical and pleiotropic actions of dipyridamole: Not enough light to illuminate the dark tunnel? *Pharmacological research* **87**, 144-150, doi:10.1016/j.phrs.2014.05.008 (2014).

Figures legends

Figure 1. NHP2L1 expression and sensitivity of primary B leukemic cells to vincristine. NHP2L1 mRNA expression was determined by Affymetrix gene expression array. MTT was used to determine the sensitivity of primary cells to vincristine. The association between log2 expression of NHP2L1 and vincristine sensitivity was assessed in two cohorts of patients with acute lymphoblastic leukemia: (a) St. Jude Children's Research Hospital and (b) DCOG/COALL cohorts. Based on previously published criteria24 sensitive cells were defined as having a vincristine concentration lethal to 50% of the cells (LC50) of 0.391 μg /ml (0.474 μM) or less, and resistant cells were defined as having an LC50 of 1.758 μg/ml (2.131 μM)or more. The horizontal line inside each box depicts the median, the upper and lower limits of the box are the 75th and 25th percentiles, respectively, and the vertical bars above and below each box indicate the maximum and minimum values, respectively. P values were determined by linear regression comparing NHP2L1 gene expression and leukemia cell sensitivity to vincristine.

Figure 2. Knockdown of NHP2L1 and sensitivity to vincristine and mitotic arrest in leukemic cell lines. Human leukemia cells infected with two different shRNAs against NHP2L1 show a decrease in NHP2L1 protein levels in CCRF-CEM (a and in NALM6 (c). After knockdown of NHP2L1 cells were treated for 72 hours in the presence of increasing concentrations of vincristine. Vincristine sensitivity (LC_{50}) Cell viability determined by MTT in CCRF-CEM (b) and in NALM6 (d) are represented. Error bars represent standard deviations of three replicate experiments. Student's t-test was used to calculate *P-values*. * P<0.05, ** P<0.01, *** P<0.001. Human leukemia cells (CCRF-CEM and NALM6) were infected with two different shRNAs (#1, #2) against NHP2L1 and treated with vincristine for 24 hours. Representative blots of phosphorylated Serine 10 in Histone H3 protein and of total Histone H3 after knockdown of NHP2L1 and 24 hours treatment with vincristine were shown in CEM (e) and NALM6 cells (g). Phospho Histone H3 protein levels were quantified by densitometry, normalized to Total Histone H3 signal and expressed in arbitrary units for the CEM cells (f) and for the NALM6 cells (h). Values are means ± SD of three independent experiments. Student's t-test was used to calculate *P-values.* * P<0.05, ** P<0.01, *** P<0.001.

Figure 3. Effects of small molecules inhibitors of NHP2L1 U4 interaction on neurons and leukemic cells treated with vincristine. (a) Vincristine (VCR) effects relative to dipyridamole (DIP) on neurons and two ALL cell lines (CEM and NALM6). The y-axis represents the ratio of the additive EC_{50} to the actual EC_{50} for the combination of VCR and DIP. Each bar represents a fixed concentration of DIP [0.25 µM (0.125 mg/L), 0.5 µM (0.25 mg/L), 1 µM (0.5 mg/L), 2.5 µM (1.265 mg/L), 5 µM (2.525 mg/L), and 10 µM (5.05 mg/L)]. The whiskers are the 95% confidence interval of the measure. A ratio of one indicates the combination is additive while a ratio greater or less than one indicates that the combination is either synergistic or antagonistic, respectively. (b) Representative images of human iPSC neurons (Peri.4U) 72 hours after treatment with increasing concentrations of vincristine with or without increasing concentrations of dipyridamole. Images were taken from the ImageXpress Micro imaging microscope at 10x magnification.

Figure 4. Effects of dipyridamole on vincristine-induced mitotic arrest and on SORORIN protein level.

Human leukemia cells (CCRF-CEM and NALM6) were treated with vincristine [2nM (1.65 μg/L)] for 24 hours alone or with increasing concentrations of dipyridamole. Representative blots of phosphorylated Serine 10 in Histone H3 protein and of total Histone H3 after 24 hours treatment with vincristine and increasing concentrations of dipyridamole for human ALL cell lines CEM (a) and NALM6 (c) are shown. Phospho Serine 10 Histone H3 protein levels were quantified by densitometry, normalized to Total Histone H3 signal and expressed in arbitrary units for the CEM cells (b) and for the NALM6 cells (d). Values are means ± SD of three independent experiments. Student's t-test was used to calculate *P-values*. * P<0.05, ** P<0.01, *** P<0.001. G2 synchronized cells where treated with increasing concentration of dipyridamole, and expression of SORORIN was document by western blot in CEM (e) and NALM6 (g) cells. The level of SORORIN was normalized to the level of GAPDH and the ratio was plotted for the CEM (f) and the NALM6 (h) cells. Values are means ± SD of three independent experiments. Student's t-test was used to calculate *P-values*. * P<0.05, ** P<0.01, *** P<0.001.

Figure 5. Intracellular concentration of vincristine or dipyridamole in CEM human leukemia cell line, or hiPSC-derived neurons relative to incubation time (hours) and vincristine neurotoxicity in mice. Intracellular concentration of vincristine was determined in (a) CEM ALL cells after exposure of the cells to 2nM (1.65 μg/L) or 40nM (33 μg/L) of vincristine with or without increasing concentrations of dipyridamole: 0μM in black, 2.5μM (1.265 mg/L) in blue, 5μM (2.525 mg/L) in green and 10μM (5.05 mg/L) in magenta. The circles and whiskers represent the median and range of the data. The ΔV_{max} represents the change in Vmax due to the presence of dipyridamole. The *p-values* test whether the change in V_{max} (ΔV_{max}) due to the presence of dipyridamole differs from 0 using the t-test (a). Intracellular concentration of dipyridamole was determined in (b) CEM after treating leukemia cells with 2.5 μM (1.265 mg/L), 5 μM (2.525 mg/L), or 10 μM (5.05 mg/L) of dipyridamole with or without increasing concentrations of

vincristine: 0 nM in black, 2 nM (1.65 μg/L) in blue and 40 nM (33 μg/L) in green. The circles and whiskers represent the median and range of the data. The *p-values* test whether the change in the slope due to the presence of vincristine is different from 0 using the t-test (b). Intracellular levels of dipyridamole were not significantly related to extracellular vincristine concentrations. Intracellular concentration of vincristine was determined in hiPSC-derived neurons after treatment of the cells with 40 nM (33 μg/L) of vincristine with or without 5 μM (2.525 mg/L) of dipyridamole: 0 μM in black, 5 μM (2.525 mg/L) in blue (c). The *p-values* test if ΔV_{max} differs due to the presence or absence of dipyridamole using the t-test (c). The circles and whiskers represent the median and range of the data. The ΔV_{max} represents the change in Vmax due to the presence of dipyridamole. Intracellular concentration of dipyridamole was determined in hiPSC-derived neurons after treating the cells with 5μM of dipyridamole with or without 40 nM (33 μg/L) of vincristine: 0nM in black, and 40nM (33 μg/L) in blue. The circles and whiskers represent the median and range of the data (d) The *p-values* test whether ΔV_{max} due to the presence of vincristine is different from 0 using the t-test (d). (e) Paw withdrawal responses expressed as percentage were determined using von Frey filaments at baseline, day 7, day 10 and day 14 in mice receiving one of the following treatment: saline and vehicle of dipyridamole; saline and dipyridamole; vincristine and vehicle of dipyridamole; vincristine and dipyridamole. (f) Cross-sectional and cumulative proportion (CPN) of mice positive for neurotoxicity in each treatment group is depicted. Positive neurotoxicity was defined as values higher than 95th percentile of the von Frey measurements. (g) NSG mice were inoculated with human CEM leukemia cells. After engraftment the mice were treated once a week with saline and vehicle (controls), vincristine, dipyridamole or the two drugs together. Percentage survival was determined for each group of mice. Mice receiving vincristine and vehicle showed a significantly prolonged survival compared to controls (saline + vehicle as well as saline + dipyridamole) (*p-value*<0.001). The addition of dipyridamole to vincristine significantly prolonged the survival of mice compared to mice treated with only vincristine and vehicle (*p-value*<0.001)

Tables

Table 1: Estimate of drug-drug interaction between vincristine and second drug (dipyridamole, tazarotene, and quetiapine fumarate) in CEM and NALM6 ALL cell-lines. Values of α significantly greater than zero indicate synergy and values significantly less than zero indicate antagonism. The *p-value* indicates the significance of the interaction term (α) relative to additive (0) and was determined using a *t-test*.

Drug Name	**CEM α**	**CEM *P-value***	**NALM6 α**	**NALM6 *P-value***
Dipyridamole	11.6	2.45×10^{-9}	4.45	6.9×10^{-25}
Tazarotene	0.945	9.66×10^{-7}	1.42	1.43×10^{-11}
Quetiapine fumarate	0.787	0.0235	2.33	1.73×10^{-7}

Table 2: Estimate of drug-drug interaction between vincristine and second drug (dipyridamole, tazarotene, and quetiapine fumarate) in hiPSC-derived neurons. Values of α significantly greater than zero indicate synergy and values significantly less than zero indicate antagonism. The *p-value* indicates the significance of the interaction term (α) relative to additive (0) and was determined using a *t-test*.

Drug Name	**Branches**		**Processes**		**Outgrowth**		**Viability**	
	α	*P-value*	α	*P-value*	α	*P-value*	α	*P-value*
Dipyridamole	-3.43	2.8e-12	-1.75	5.07e-09	-1.98	5.69e-08	-3.7	4.83e-11
Tazarotene	-1.16	0.032	-1.59	2.05e-08	-1.63	2.9e-07	-0.72	0.25
Quetiapine fumarate	-2.29	2.22e-07	-1.25	1.47e-04	-1.67	6.32e-06	-0.007	0.99

Figure 1

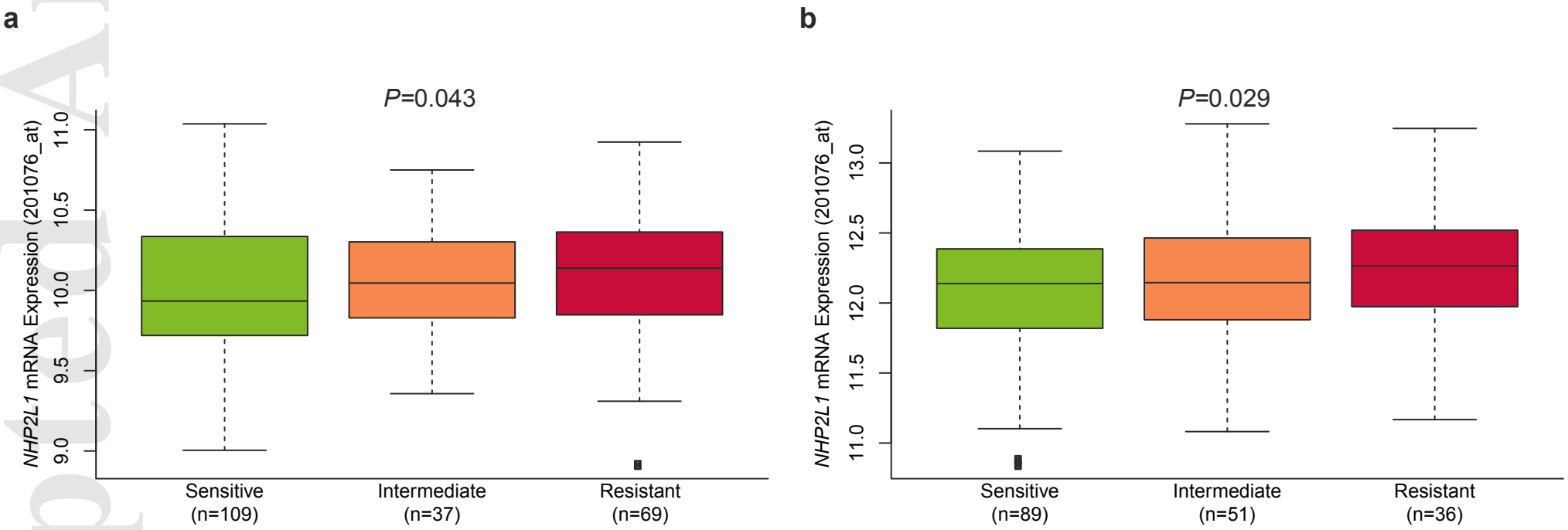

Figure 2

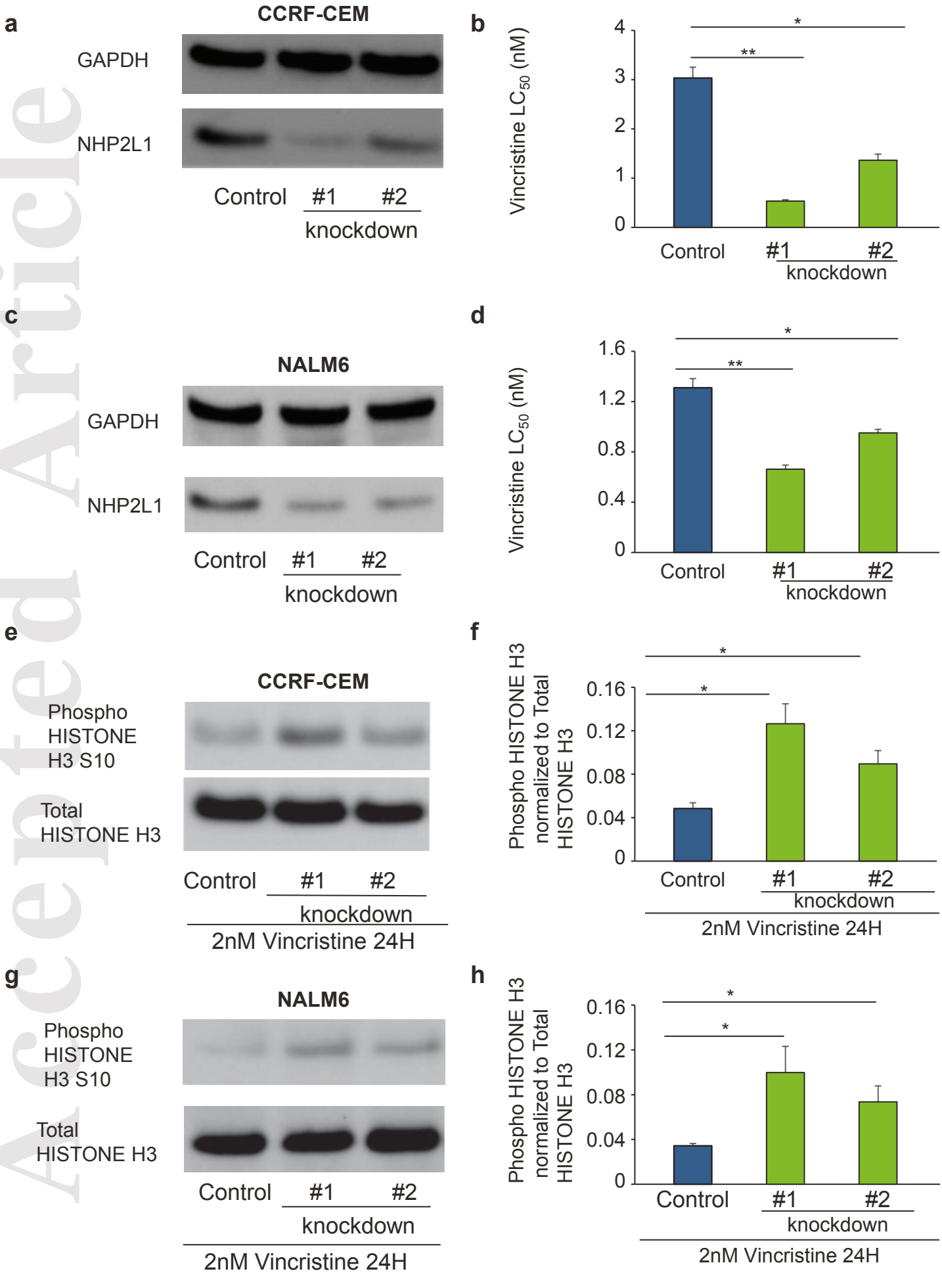

Figure 3

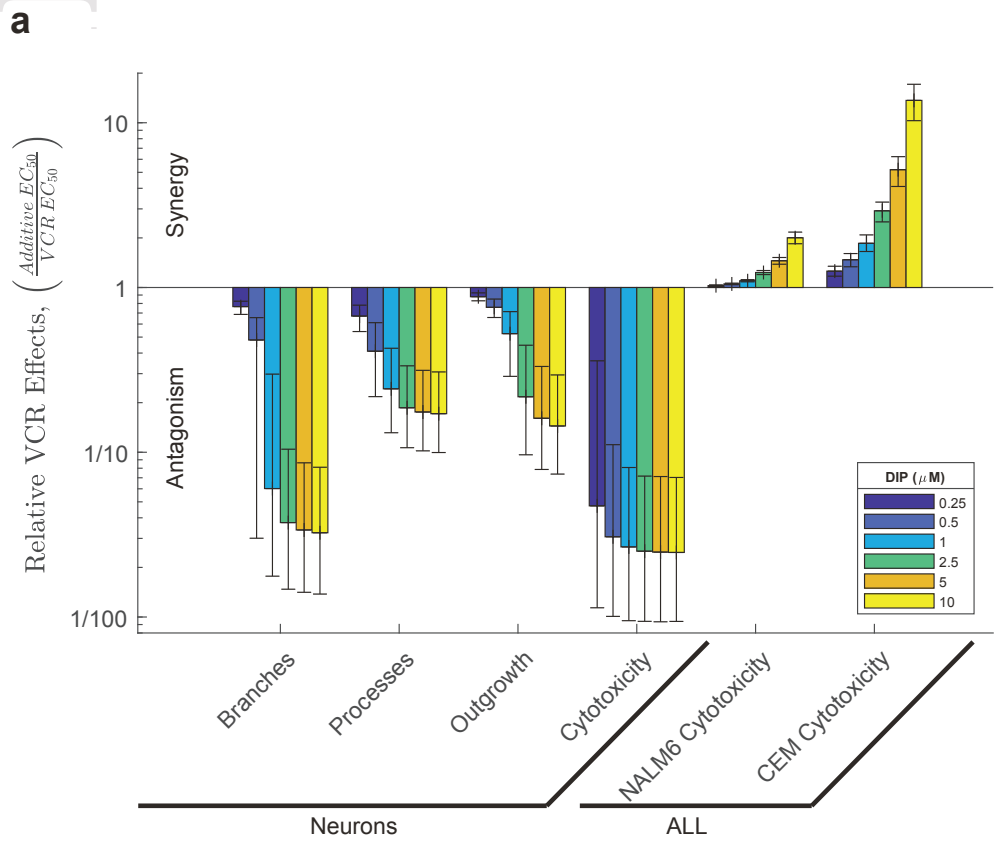
a
Relative VCR Effects, $\left(\frac{Additive\ EC_{50}}{VCR\ EC_{50}}\right)$
10
1
1/10
1/100
Synergy
Antagonism
DIP (μM)
0.25
0.5
1
2.5
5
10
Branches
Processes
Outgrowth
Cytotoxicity
NALM6 Cytotoxicity
CEM Cytotoxicity
Neurons
ALL

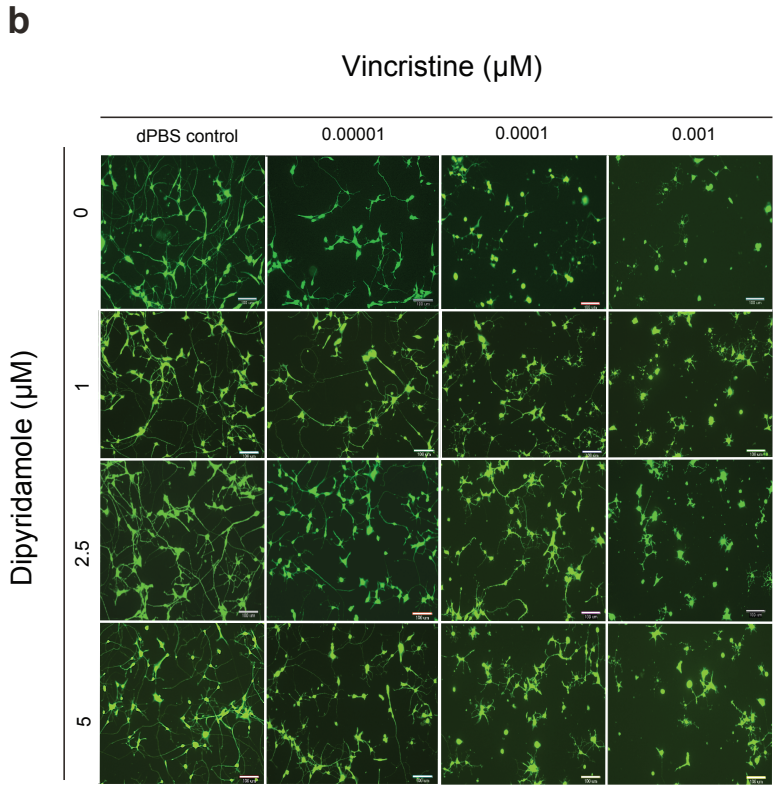
b
Vincristine (μM)
dPBS control
0.00001
0.0001
0.001
Dipyridamole (μM)
0
1
2.5
5

Figure 4

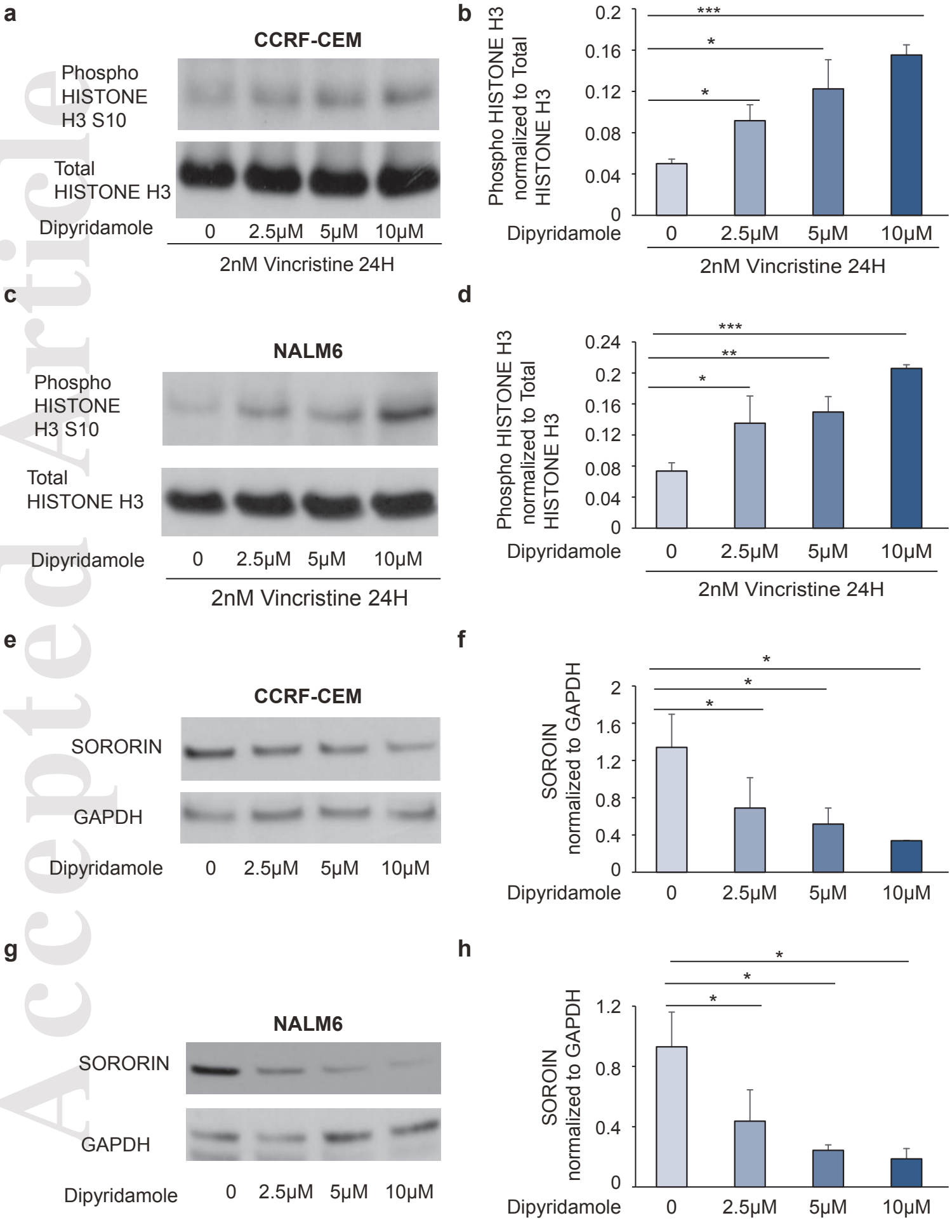

Figure 5